Chiral Complexes

Deutsche Ausgabe: DOI: 10.1002/ange.201506539
Internationale Ausgabe: DOI: 10.1002/anie.201506539

Superchiral Pd_3L_6 Coordination Complex and Its Reversible Structural Conversion into $Pd_3L_3Cl_6$ Metallocycles

Ondřej Jurček, Pia Bonakdarzadeh, Elina Kalenius,* Juha Matti Linnanto, Michael Groessl, Richard Knochenmuss, Janne A. Ihalainen, and Kari Rissanen**

Abstract: *Large, non-symmetrical, inherently chiral bispyridyl ligand* ***L*** *derived from natural ursodeoxycholic bile acid was used for square–planar coordination of tetravalent* Pd^{II}*, yielding the cationic single enantiomer of superchiral coordination complex* ***1*** Pd_3L_6 *containing 60 well-defined chiral centers in its flower-like structure. Complex* ***1*** *can readily be transformed by addition of chloride into a smaller enantiomerically pure cyclic trimer* ***2*** $Pd_3L_3Cl_6$ *containing 30 chiral centers. This transformation is reversible and can be restored by the addition of silver cations. Furthermore, a mixture of two constitutional isomers of trimer,* ***2*** *and* ***2′****, and dimer,* ***3*** *and* ***3′****, can be obtained directly from* ***L*** *by its coordination to trans- or cis-N-pyridyl-coordinating* Pd^{II}*. These intriguing, water-resistant, stable supramolecular assemblies have been thoroughly described by* ^1H *DOSY NMR, mass spectrometry, circular dichroism, molecular modelling, and drift tube ion-mobility mass spectrometry.*

Chirality is a common property of many naturally occurring compounds and an essential element of life. In the field of supramolecular chemistry, there have been significant efforts to mimic Nature in the preparation of chiral concave supramolecular systems utilizing chiral natural products, their derivatives, or various synthetic ligands. Chiral cavity-containing structures are attractive for a variety of applications, from transport and recognition to catalysis and protection of biochemically active and inherently chiral compounds. Supramolecular chemistry can utilize various reversible and irreversible intermolecular interactions to obtain concave assemblies. One of the most fascinating strategies, which results in directed and stable interaction between the subunits, is to utilize the coordination ability of organic binding sites to metals, forming either distinct metallo-supramolecular structures (capsules, cages, or other assemblies having cavities)[1] or polymeric materials (metal–organic frameworks, or MOFs).[2]

The coordination geometry of the metal ions and the number of the binding sites of the ligands and overall structure of the ligand define geometry of the coordination assembly. The use of divalent or tetravalent Pd^{II} of *cis*-, *trans*-, or square–planar binding geometry, together with various rigid or flexible pyridyl ligands, has proven to be a successful strategy in obtaining numerous supramolecular assemblies. In general, the ligands used for their preparation are mostly symmetrical, relatively rigid, and very often achiral.[1]

To prepare discrete chiral species of Pd^{II} or Pt^{II}, two pathways have been developed: i) utilization of chiral metallo-corners and achiral ligands, or ii) chelation of chiral multidentate ligands to achiral metals. In the second case, the chiral moiety might be appended to a side of the ligand,[3] or a simple chiral molecule can constitute the actual core of the ligand.[4]

Focusing on the chiral concave coordination assemblies resembling the structures presented and starting from the smallest ones, several examples of chiral metallo-supramolecular rhomboids have been prepared by self-assembly of chiral bis-pyridyl-substituted ditopic ligands with 90° *cis*-blocked Pd^{II}, often with $[(enPd)(NO_3)_2]$.[5] There are no chiral supramolecular triangles described so far, but a large number of their achiral analogues.[1a,c] And finally, the preparation of large achiral molecular open boxes, either trifacial or multi-facial, can be done through self-assembly of di- or tetratopic ligands and 90° building blocks. The trifacial box is the smallest and entropically the most preferred isomer, which can be represented by either assembly M_6L_3 or M_3L_6. For the former assembly, the organic linker is often tetrapyridyl coordinating to 90° Pt or Pd metal corners.[6,7] The M_3L_6 assembly is represented by work of Fujita et al., where 60° donor, 1,2-bis(ethynylpyridine)benzene, in combination with Pd^{II}, yielded solvato-controlled assemblies of Pd_3L_6 and Pd_4L_8.[8a] Clever et al. described an intertwined achiral Pd_3L_6 cage built of two trefoil-knotted substructures.[8b] However, chiral concave structures of Pd_3L_6 have not yet been obtained.

Small terpenoids have been used on several occasions for modification of coordination ligands,[9] yet large triterpenoids, such as bile acids, have not been utilized for preparation of the ligand itself. Bile acids are inexpensive, natural, and enantiomerically pure compounds (with over 9 chiral centers in

[*] Dr. O. Jurček, P. Bonakdarzadeh, Dr. E. Kalenius, Prof. K. Rissanen
University of Jyvaskyla
Department of Chemistry, Nanoscience Center
P.O. Box 35, 40014 University of Jyvaskyla (Finland)
E-mail: jurcekondrej@gmail.com
elina.o.kalenius@jyu.fi
kari.t.rissanen@jyu.fi
Dr. J. M. Linnanto
University of Tartu, Institute of Physics
Ravila 14c, 50411 Tartu (Estonia)
Dr. M. Groessl, Dr. R. Knochenmuss
Tofwerk AG
Uttigenstrasse 22, 3600 Thun (Switzerland)
Prof. J. A. Ihalainen
University of Jyvaskyla, Nanoscience Center
Department of Biological and Environmental Science
P.O. Box 35, 40014 University of Jyvaskyla (Finland)

Supporting information for this article is available on the WWW under http://dx.doi.org/10.1002/anie.201506539.

 © 2015 Wiley-VCH Verlag GmbH & Co. KGaA, Weinheim

a single molecule). Their rigid tetracyclic steroid skeleton is decorated by various numbers of readily reactive hydroxy groups of defined stereochemistry, and by flexible alkyl chains bearing carboxyl functional groups, which makes them excellent building blocks for supramolecular and material chemistry.[10,11] Several groups of covalent macrocycles built of 2–5 bile acid units have been presented and studied for their host–guest chemistry, for example, cyclocholates, cholaphanes, and cyclocholamides.[10,12] Nevertheless, large macrocyclic bile acid-based systems have not been built by metal-coordination. Out of available bile acids, only ursodeoxycholic acid (UDCA) provides an optimal conformation of the hydroxy groups (position 3*R*,7*S* in divergent manner) containing 110° angles, which can be further equipped by pyridyl binding sites. For these reasons, UDCA was selected as the starting building block for the preparation of our ligand when aiming at the construction of superchiral coordination complexes.

The ligand **L** was prepared in two steps from UDCA (Scheme 1). Complexation of **L** with $[Pd(CH_3CN)_4(BF_4)_2]$ in

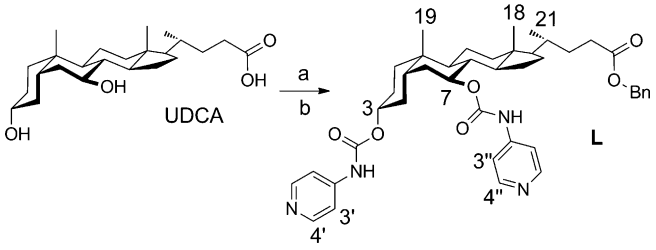

Scheme 1. Preparation of ligand **L**. Reaction conditions: a) potassium bicarbonate, DMF, benzyl bromide; b) triphosgene, pyridine, CH_2Cl_2.

2:1 ratio in $[D_6]$DMSO (55 °C, 15 min) provided supramolecular assembly **1**, $Pd_3\mathbf{L}_6$. From the ^{1}H NMR spectrum, clear downfield chemical shifts of the carbamate -NH- protons and pyridyl β-protons (H3′ and H3″), and slight upfield shift of pyridyl α-protons (H4′ and H4″) were attributed to a successful and quantitative metal–ligand complexation (Figure 1). The number of signals for the complex corresponds to those of the ligand, indicating that the supramolecular assembly is formed spontaneously in symmetrical and precise order.

Based on the symmetry of **1**, there are two options for the ligand assembly around the Pd metal centers. The $Pd_3\mathbf{L}_6$ complex can be assembled by clockwise- and counterclockwise-directed three-membered ligand cycles aligned in 3→7 connectivity (barrel shape, numbering in Scheme 1; Supporting Information, Figure S5), or of two parallel clockwise cycles aligned similarly 3→7 (flower shape, Figure 2). In both cases the cycles are interconnected through coordination to three atoms of square–planar Pd^{II} (PdN_4 coordination sphere). The comparison of their ground state energies of optimized molecular models $E_{flower} < E_{barrel}$ ($\Delta E = 20$ kcal. mol^{-1}) suggests preferential formation of the flower-like complex (Figures 2, S5).

ESI-MS analysis of **1** shows an intense single peak corresponding to ion $[Pd_3\mathbf{L}_6]^{6+}$ (Figure 3). The drift tube IM-MS analysis for $[Pd_3\mathbf{L}_6]^{6+}$ shows the presence of several

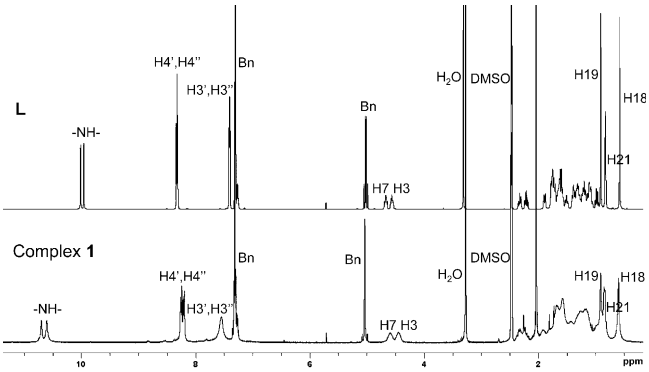

Figure 1. Formation of hexamer **1** from **L** as followed by ^{1}H NMR ($[D_6]$DMSO, 400 MHz, 298 K).

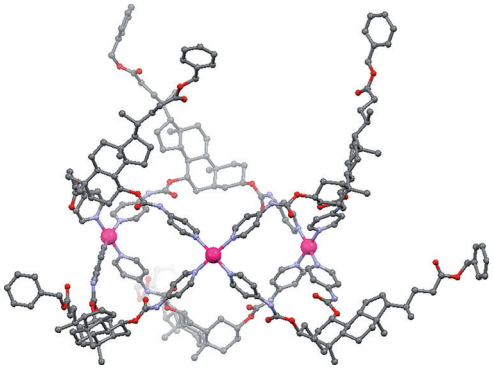

Figure 2. Optimized structures of **1** (CAM-B3LYP, hydrogens were omitted for clarity).

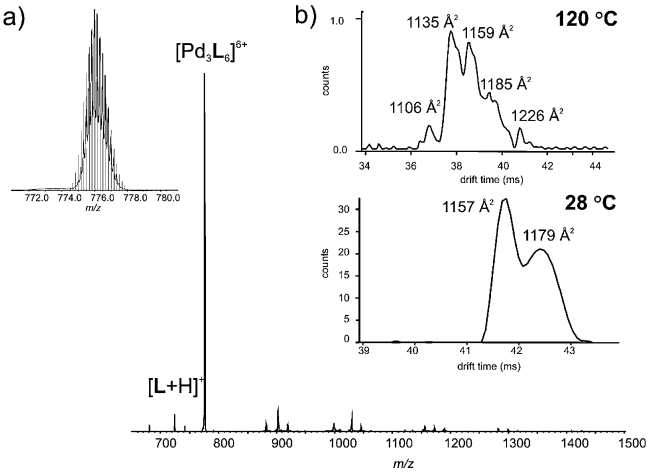

Figure 3. a) ESI-TOF MS spectrum from **1** (5 μM in CH_3CN). Inset shows the fit of theoretical isotopic distribution for ion at *m/z* 776 which corresponds to molecular formula of $[Pd_3\mathbf{L}_6]^{6+}$. b) IM-MS ion mobilograms for ion $[Pd_3\mathbf{L}_6]^{6+}$ recorded at drift tube temperatures 120 °C and 28 °C.

closely related conformers of **1**, which can be seen by the different, yet close, drift times. Their distribution results from variation of collision cross-sections (CCSs) for particular conformers between 1106 and 1192 Å^2, corresponding to the

 © 2015 Wiley-VCH Verlag GmbH & Co. KGaA, Weinheim

maximum of 10 Å difference in CCS derived diameters (if a spherical structure for the complex was assumed). The conformational diversity is temperature-dependent and is likely caused by the movements of the flexible alkyl side chains bearing benzyl carboxylate group, which might resemble "waving" of the complex (or possibly opening and closing of the flower). Close to RT there are only two gas-phase conformers observed, but at elevated temperature of 120 °C at least 10 distinct conformers can be seen (Figure 3).

Spatial movement of the benzyl groups can also be observed from multiple ^{13}C NMR signals corresponding to benzyl carbons (Figures S7, S8b). Broadening and multiplicity of the carbon signals in the upper side of the steroid skeleton (C11, C18, C19, and C21) can be assigned to the interaction with the surrounding benzyl groups, or possible formation of their self-inclusion complex (Figure S8a). Furthermore, the ^1H NMR spectrum of **1** at 130 °C excludes the possibility that the IM-MS profile observed could originate from different isomers and not from different conformers as suggested (Figure S6). Unfortunately, the motion of benzyl groups might also be the reason for the difficulties in obtaining an X-ray quality single crystal of **1**. Moreover, the ^{13}C NMR spectrum revealed four different signals for CH_3CN of the palladium salt (Figures S7, S8a), which presents an initial implication on the ability of **1** to operate in host–guest chemistry.

^1H DOSY NMR measurements show that all the proton signals originate from one species with diffusion coefficient $D = 6.73 \times 10^{-11}\ m^2 s^{-1}$ ($\log D = -10.17$, [D_6]DMSO, 303 K; Figure S9). This value corresponds to the hydrodynamic diameter of 3.6 nm, as calculated from the Stokes–Einstein equation under the consideration of its roughly spherical shape. This value is in good agreement with the calculated 3.8 nm diameter obtained from the CCS acquired by IM-MS measurement and with the 3.9 nm diameter determined from its molecular model.

Circular dichroism (CD) studies of **L** and **1** were performed to examine their chirality. The CD spectra were compared with those calculated from their optimized structures in methanol (Figure 4 for **1**, Figure S36 for **L**). Calculated spectra reproduce the overall structures of the experimental CD spectra, indicating that structural models are realistic. CD bands at around 240 nm are shifted to the 260 nm, owing to the formation of the coordination structure/bond. Similar shifts can be observed also from the UV/Vis absorption spectra of **L** and **1** (Figure S33). The experimental CD spectrum of **1** shows a negative shoulder in the low energy side of the 270 nm band, and a very weak positive band at about 330 nm. Calculations produce the weak 330 nm band but underestimate the negative shoulder. For more details, see the Supporting Information, Chapter 3.

Complex **1** was further studied for its stability in aqueous solution by MS (**1** measured from H_2O, Figure S11), and by ^1H NMR titration with D_2O (Figure S10). Both methods showed **1** to be robust and water-stable. Interestingly, the addition of D_2O into 10 mM [D_6]DMSO solution in a 1:3 ratio resulted in the formation of a gel.

Complex **1** can readily be transformed to a single constitutional isomer of trimer $Pd_3\mathbf{L}_3Cl_6$ (reaction pathway 1, *RP1*;

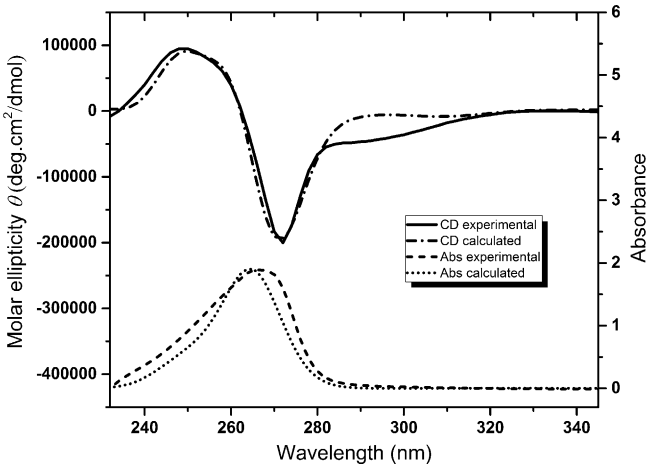

Figure 4. Comparison of experimental and simulated CD and UV/Vis spectra of **1**.

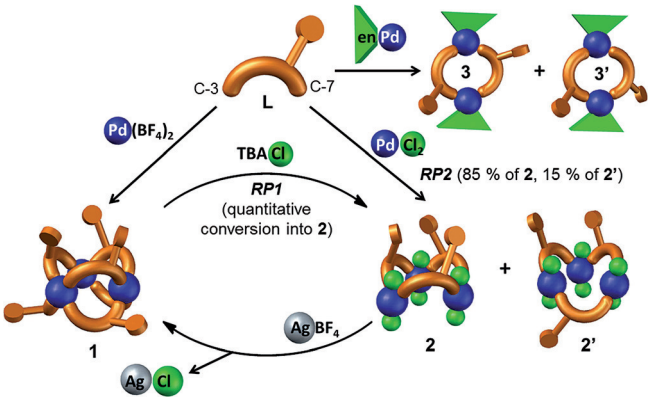

Scheme 2. General preparation and interconversion of coordination assemblies of **L**.

Scheme 2) by treatment with alkylammonium chlorides (TMACl or TBACl). Six chloride anions replace three molecules of **L** during this transformation, giving Pd complex of the PdN_2Cl_2 coordination sphere. After the saturation point is reached, complex **2** remains stable even at higher concentrations of TBACl, as shown by ^1H NMR (Figure S12). Observation of a single isomer **2** in ^1H NMR spectrum is further support for assembly **1** to be the flower-like assembly (from two clockwise cycles connected through PdN_4, **1**; by addition of Cl^- we obtain one clockwise cycle of **L**s coordinating as *trans*-PdN_2Cl_2 sphere, **2**).

^1H DOSY NMR experiments show assembly with $D = 7.15 \times 10^{-11}\ m^2 s^{-1}$ ([D_6]DMSO, 303 K) for complex **2**, which corresponds to a complex that is larger than **L** yet smaller than **1** (for comparison, see Table 1). This could be assigned to two possible assemblies $Pd_2\mathbf{L}_2Cl_4$ or $Pd_3\mathbf{L}_3Cl_6$. The final product **2** cannot be observed directly by ESI-MS because of its zero net charge. Instead, an MS experiment was designed to follow the stepwise formation of **2** by measuring the reaction mixture after partial additions of TMACl to the solution of **1**. Indeed, by this approach gradual and fast (within minutes) formation of $[Pd_3\mathbf{L}_5Cl_2]^{4+}$ and $[Pd_3\mathbf{L}_4Cl_4]^{2+}$ ions, most likely turning in

© 2015 Wiley-VCH Verlag GmbH & Co. KGaA, Weinheim

Table 1: Comparison of the results of IM-MS and ^{1}H DOSY NMR of determination of their size characteristics.

Complex	Ion	CCS [Å^2]	D [$\times 10^{-11}$ m^2 s^{-1}]
L	–	276	21.9
3 + **3′**	$[(enPd)_2\mathbf{L}_2]^{4+}$	679	8.38
2	$[Pd_3\mathbf{L}_5Cl_2]^{4+}$	879	–
	$[Pd_3\mathbf{L}_4Cl_4]^{2+}$	688	–
	$[Pd_3\mathbf{L}_3Cl_6]^0$	–	7.15
1	$[Pd_3\mathbf{L}_6]^{6+}$	1165	6.73

the next step into $[Pd_3\mathbf{L}_3Cl_6]^0$, could be detected (Figures S13, S14). The formation of $[Pd_2\mathbf{L}_2Cl_2]^{2+}$ or a similar intermediate that could lead to the complex $[Pd_2\mathbf{L}_2Cl_4]^0$ were absent. Interestingly, species having an odd number of chlorides were not observed, thus the ligand leaves in one step from both metal coordination sites, and is immediately replaced by a pair of chlorides. The IM-MS analysis for $[Pd_3\mathbf{L}_5Cl_2]^{4+}$ and $[Pd_3\mathbf{L}_4Cl_4]^{2+}$ ions show a gradual decrease in their CCS values, and cross sections of 879 Å^2 and 688 Å^2 are obtained for the main conformers (Table 1, Figure S13).

The transformation of **1** into **2** is reversible and the original structure of **1** can be restored by adding Ag^+ ions. The addition of 6 equiv of $AgBF_4$ to the sample of **2** obtained by *RP1* led to an immediate change in the ^{1}H NMR spectra, and further heating of the mixture (55 °C, 15 min) resulted in total recovery of **1** (Figure 5). Respectively, addition of $AgBF_4$ into *RP1* ESI-MS sample led to reconstruction of **1** and appearance of the peak for $[Pd_3\mathbf{L}_6]^{6+}$ (Figure S15).

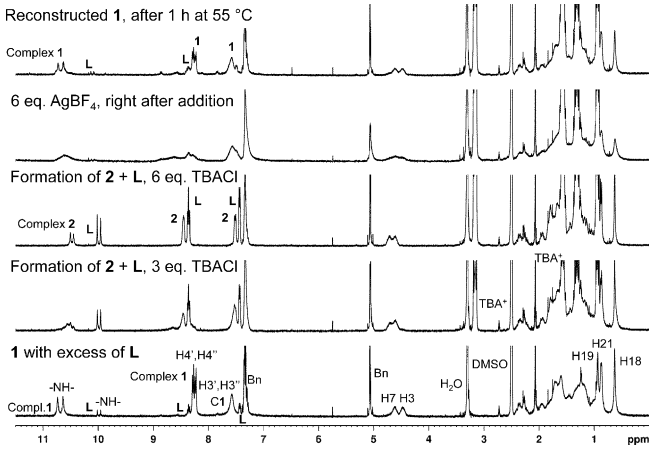

Figure 5. ^{1}H NMR spectra visualizing interconversion of **1** and **2** (from down to top). The ligand **L** was added in slight excess to compare the signals to a side-product of transformation during TBACl addition.

To provide further evidence supporting the interpretation of **2** as $Pd_3\mathbf{L}_3Cl_6$, and to fully exclude the possibility for **2** to be a dimeric assembly, we used *cis*-blocked Pd^{II} $[(enPd)(NO_3)_2]$ for complexation with **L** in 1:1 ratio. As expected from the coordination geometry of the metal, this procedure led to a formation of two constitutional isomers of dimeric $[(enPd)_2\mathbf{L}_2]^{4+}$ complexes **3** and **3′** (Figure 6; see the Supporting Information for more details). Comparison of ^{1}H DOSY NMR and CCS from IM-MS for assemblies **2** and **3** shows

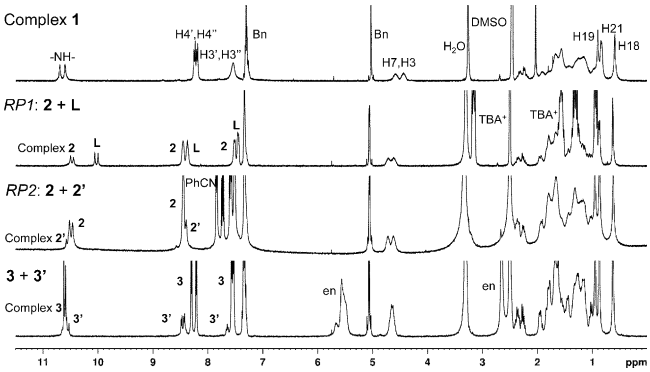

Figure 6. Comparison of ^{1}H NMR spectra for coordination assemblies **1** $Pd_3\mathbf{L}_6$, **3** and **3′** $(enPd)_2\mathbf{L}_2$, and **2** and **2′** $Pd_3\mathbf{L}_3Cl_6$ (product obtained either by the *RP1* or *RP2* pathways).

clear size differences (Table 1), which confirms the interpretation of **2** to be the trimeric complex.

The trimeric assembly **2** can also be obtained by a second reaction pathway (*RP2*), which proceeds directly from **L** by its coordination to *trans*-Pd^{II} $[(PhCN)_2PdCl_2]$ in 1:1 ratio. Beside the ^{1}H NMR signals for **2** as the main product (the same chemical shifts, as in the case of the *RP1* product), there is a very close second set of signals of a co-product **2′** (Figure 6).

From the ^{1}H DOSY NMR experiments, we can conclude that **2′** and **2** are of the same size (Figure S21). Considering the fact that the *trans*-Pd^{II} is thermodynamically more stable than its *cis*-isomer (and thus their interconversion is not viable), two different constitutional isomers, **2** and **2′**, of $Pd_3\mathbf{L}_3Cl_6$ coordination complex can be presumed (Scheme 2). Their ratio was determined as **2**:**2′** = 4:1 from the integration of ^{1}H NMR signals and our conclusions based on the isomeric distribution was confirmed by comparison of the ground state energies of their optimized molecular models, $E_{\mathbf{2}} < E_{\mathbf{2'}}$ ($\Delta E =$ 4.4 kcal.mol^{-1}; Figure S18). Thus **2** should be present in excess. Variable temperature (VT) ^{1}H NMR experiments were carried out to study the thermodynamic equilibrium between **2** and **2′** (Figure 7). The thermodynamic data obtained from the van 't Hoff plot (Supporting Information, Figure S25) are in agreement with those obtained by computational calculations and help explain the conversion (Supporting Information, Section 2.5.2).

If the ^{1}H NMR spectra of products obtained by *RP1* and *RP2* are compared (Figure 6), in the case of *RP1* there is only one set of signals corresponding to trimeric structure **2** (3→7 connectivity). This uniform directional organization can easily be explained as described above based on the organization of the parental complex **1** (both cycles are of the same directionality, thus giving the same directional single trimeric cycle after the addition of chloride). On the contrary, from the *RP2* reaction pathway we can obtain both isomers **2** and **2′** as they are formed from free ligands coordinating to *trans*-Pd^{II} in 3→7 or 7→3 connectivity.

Similar to *RP1*, the assemblies **2** and **2′** obtained by *RP2* convert to **1** in the presence of Ag^+ salt. Comparison on the ongoing chemistry of the reverse conversion for both cases can be done (Scheme 3). In the case of *RP2*, two molecules of trimer are needed for the formation of one molecule of **1**, as

 © 2015 Wiley-VCH Verlag GmbH & Co. KGaA, Weinheim

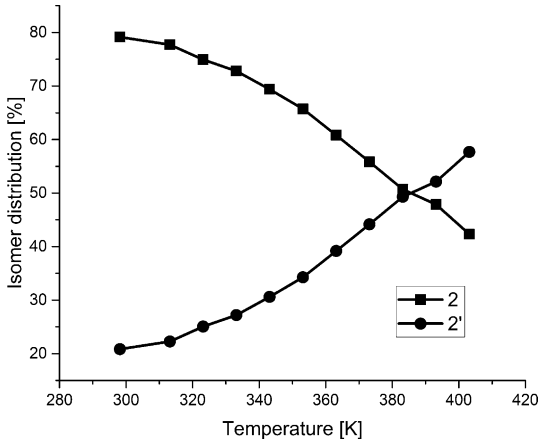

Figure 7. Changes in distribution of isomer **2** and **2′** in dependence on temperature as observed from VT ^{1}H NMR measurement.

Formation of **1**: $6\,\mathbf{L} + 3\,Pd(BF_4)_2 \rightarrow Pd_3\mathbf{L}_6^{6+} + 6\,BF_4^-$

RP1, **2**: $Pd_3\mathbf{L}_6^{6+} + 6\,Cl^- \rightarrow Pd_3\mathbf{L}_3Cl_6 + 3\,\mathbf{L}$

RP2, **2** + **2'**: $3\,\mathbf{L} + 3\,PdCl_2 \rightarrow Pd_3\mathbf{L}_3Cl_6$

RP1 → **1**: $Pd_3\mathbf{L}_3Cl_6 + 3\mathbf{L} + 6\,Ag^+ \rightarrow Pd_3\mathbf{L}_6 + 6\,AgCl$

RP2 → **1**: $2\,Pd_3\mathbf{L}_3Cl_6 + 6\,Ag^+ \rightarrow Pd_3\mathbf{L}_6 + 6\,AgCl + 3\,PdCl_2$

Scheme 3. Summary of transformation reactions of coordination assemblies of **L**.

there are no free ligands present for the direct recovery as in the case of *RP1*. This might suggest that the coordination bonds between the ligands and metals in products of *RP2* are partially broken down first, giving the building blocks for re-assembly into **1** in the second step. The same mode might also be present in *RP1* case.

Altogether, these experiments represent a nice example of reversible transformation of supramolecular systems **1** and **2** back and forth (Scheme 2).

To conclude, since the introduction of the first metallo-supramolecular squares in 1990[13] the ligands used in formation of bordered supramolecular assemblies were only symmetrical and mostly achiral. This work introduces the first successful utilization of a ligand which is non-symmetric and at the same time inherently chiral, ultimately forming an unprecedented example of enantiomerically pure metallosupramolecular coordination assembly with a record 60 chiral centers in its structure. Despite the complexity, flexibility, and number of functional groups of the ligand we find it very intriguing that the coordination complex is formed in such a unique three-fold symmetry manner. Using Pd^{II} of *trans*- or *cis*- coordination geometry we were able to prepare even smaller dimeric and trimeric metallocycles containing 20 and 30 chiral centers. Utilization of these non-symmetric chiral and relatively flexible ligands represents a new approach to stable Pd^{II} complexes with potential for a broad spectrum of applications in chiral host–guest recognition, enantioselective separation, chiral catalysis or even in applications as membrane channels owing to their amphiphilic character and likely biocompatibility. Their significant stability in aqueous environment only supports the potential for biological applications. The studies on their host–guest recognition properties are currently ongoing in our lab.

Acknowledgements

We thank to Academy of Finland (KR: proj. no. 263256 and 265328, EK: no. 284562 and 278743), University of Jyväskylä, and Estonian Research Council (JML: Grant IUT02-28) for financial support. Johanna Lind and Esa Haapaniemi are gratefully acknowledged for the help with MS and NMR. Emer. Prof. Erkki Kolehmainen is gratefully acknowledged for allowing OJ to carry out some preliminary experiments on this topic during his Ph.D. studies. Dr. Ralf Troff is acknowledged for initial MS measurement of a similar system.

Keywords: bile acid · chirality · metallocycle · self-assembly · supramolecular chemistry

How to cite: *Angew. Chem. Int. Ed.* **2015**, *54*, 15462–15467
Angew. Chem. **2015**, *127*, 15682–15687

[1] a) T. R. Cook, P. J. Stang, *Chem. Rev.* **2015**, *115*, 7001–7045; ; b) T. K. Ronson, S. Zarra, S. P. Black, J. R. Nitschke, *Chem. Commun.* **2013**, *49*, 2476–2490; c) R. Chakrabarty, P. S. Mukherjee, P. J. Stang, *Chem. Rev.* **2011**, *111*, 6810–6918; d) M. D. Ward, *Chem. Commun.* **2009**, 4487–4499; e) R. W. Saalfrank, H. Maid, A. Scheurer, *Angew. Chem. Int. Ed.* **2008**, *47*, 8794–8824; *Angew. Chem.* **2008**, *120*, 8924–8956; f) S. R. Seidel, P. J. Stang, *Acc. Chem. Res.* **2002**, *35*, 972–983; g) D. L. Caulder, C. Brückner, R. E. Powers, S. König, T. N. Parac, J. A. Leary, K. N. Raymond, *J. Am. Chem. Soc.* **2001**, *123*, 8923–8938; h) P. J. Stang, B. Olenyuk, *Acc. Chem. Res.* **1997**, *30*, 502–518; i) S. J. Lee, W. Lin, *Acc. Chem. Res.* **2008**, *41*, 521–537; j) M. Han, D. M. Engelhard, G. H. Clever, *Chem. Soc. Rev.* **2014**, *43*, 1848–1860.

[2] a) T. R. Cook, Y.-R. Zheng, P. J. Stang, *Chem. Rev.* **2013**, *113*, 734–777; b) B. Kesanli, W. Lin, *Coord. Chem. Rev.* **2003**, *246*, 305–326; c) H. Furukawa, K. E. Cordova, M. O′Keeffe, O. M. Yaghi, *Science* **2013**, *341*, 974–986.

[3] a) N. Kamiya, M. Tominaga, S. Sato, M. Fujita, *J. Am. Chem. Soc.* **2007**, *129*, 3816–3817; b) M. Ikemi, T. Kikuchi, S. Matsumura, K. Shiba, S. Sato, M. Fujita, *Chem. Sci.* **2010**, *1*, 68–71.

[4] a) C. Klein, C. Gütz, M. Bogner, F. Topić, K. Rissanen, A. Lützen, *Angew. Chem. Int. Ed.* **2014**, *53*, 3739–3742; *Angew. Chem.* **2014**, *126*, 3814–3817; b) R. Hovorka, S. Hytteballe, T. Piehler, G. Meyer-Eppler, F. Topić, K. Rissanen, M. Engeser, A. Lützen, *Beilstein J. Org. Chem.* **2014**, *10*, 432–441; c) C. Gütz, R. Hovorka, C. Klein, Q.-Q. Jiang, C. Bannwarth, M. Engeser, C. Schmuck, W. Assenmacher, W. Mader, F. Topić, K. Rissanen, S. Grimme, A. Lützen, *Angew. Chem. Int. Ed.* **2014**, *53*, 1693–1698; *Angew. Chem.* **2014**, *126*, 1719–1724.

[5] a) M. Fujita, M. Aoyagi, K. Ogura, *Inorg. Chim. Acta* **1996**, *246*, 53–57; b) M. Fujita, F. Ibukuro, H. Hagihara, K. Ogura, *Nature* **1994**, *367*, 720–724; c) M. Fujita, F. Ibukuro, H. Seki, O. Kamo, M. Imanari, K. Ogura, *J. Am. Chem. Soc.* **1996**, *118*, 899–900; d) M. Fujita, F. Ibukuro, K. Yamaguchi, K. Ogura, *J. Am. Chem. Soc.* **1995**, *117*, 4175–4176.

[6] Pt^{II} corner: a) D. C. Caskey, T. Yamamoto, C. Addicott, R. K. Shoemaker, J. Vacek, A. M. Hawkridge, D. C. Muddiman, G. S. Kottas, J. Michl, P. J. Stang, *J. Am. Chem. Soc.* **2008**, *130*, 7620–7628; b) J. Vacek, D. C. Caskey, D. Horinek, R. K. Shoemaker, P. J. Stang, J. Michl, *J. Am. Chem. Soc.* **2008**, *130*, 7629–7638.

 © 2015 Wiley-VCH Verlag GmbH & Co. KGaA, Weinheim

[7] Pd^{II} corner: N. Fujita, K. Biradha, M. Fujita, S. Sakamoto, K. Yamaguchi, *Angew. Chem. Int. Ed.* **2001**, *40*, 1718 – 1721; *Angew. Chem.* **2001**, *113*, 1768 – 1771.
[8] a) K. Suzuki, M. Kawano, M. Fujita, *Angew. Chem. Int. Ed.* **2007**, *46*, 2819 – 2822; *Angew. Chem.* **2007**, *119*, 2877 – 2880; b) D. M. Engelhard, S. Freye, K. Grohe, M. John, G. H. Clever, *Angew. Chem. Int. Ed.* **2012**, *51*, 4747 – 4750; *Angew. Chem.* **2012**, *124*, 4828 – 4832.
[9] O. Mamula, A. Zelewsky, *Coord. Chem. Rev.* **2003**, *242*, 87 – 95.
[10] J. Tamminen, E. Kolehmainen, *Molecules* **2001**, *6*, 21 – 46.
[11] a) H. Svobodová, V. Noponen, E. Kolehmainen, E. Sievanen, *RSC Adv.* **2012**, *2*, 4985 – 5007; b) Nonappa, U. Maitra, *Org. Biomol. Chem.* **2008**, *6*, 657 – 669.
[12] a) R. P. Bonar-Law, J. K. M. Sanders, *J. Chem. Soc. Chem. Commun.* **1991**, 574 – 577; b) R. P. Bonar-Law, A. P. Davis, B. A. Murray, *Angew. Chem. Int. Ed. Engl.* **1990**, *29*, 1407 – 1408; *Angew. Chem.* **1990**, *102*, 1497 – 1499; c) R. P. Bonar-Law, A. P. Davis, *Tetrahedron* **1993**, *49*, 9829 – 9844; d) K. M. Bhattarai, A. P. Davis, J. J. Perry, C. J. Walter, *J. Org. Chem.* **1997**, *62*, 8463 – 8473; e) H. Gao, J. R. Dias, *New J. Chem.* **1998**, *22*, 579 – 583.
[13] M. Fujita, J. Yazaki, K. Ogura, *J. Am. Chem. Soc.* **1990**, *112*, 5645 – 5647.

Received: July 15, 2015
Revised: September 12, 2015
Published online: November 4, 2015

 © 2015 Wiley-VCH Verlag GmbH & Co. KGaA, Weinheim